

**Tectono-Climatic Controls
on Broad-Scale Patterns of Compositional Variation
in the Upper Devonian Cleveland Member
of the Ohio Shale, Central Appalachian Basin**

**Jacek Jaminski^{1,*}, Thomas J. Algeo¹,
J. Barry Maynard¹, Thomas Kuhn¹,
and James C. Hower^{2,3}**

¹H. N. Fisk Laboratory of Sedimentology
Department of Geology
University of Cincinnati
Cincinnati, OH 45221-0013

*Present address:
Amoco Exploration & Production
P.O. Box 3092
Houston, TX 77253-3092

²Center for Applied Energy Research
3572 Iron Works Pike
Lexington, KY 40511-8433

³Department of Geological Sciences
University of Kentucky
Lexington, KY 40506-0059

(In: Algeo, T.J., and Maynard, J.B. (Eds.), 1997. *Cyclic Sedimentation of Appalachian Devonian and Midcontinent Pennsylvanian Black Shales: Analysis of Ancient Anoxic Marine Systems—A Combined Core and Field Workshop*: Joint Meeting of Eastern Section AAPG and The Society for Organic Petrography (TSOP), Lexington, Kentucky, Sept. 27-28, 1997, p. 63-77.)

ABSTRACT

The Upper Devonian Cleveland Member of the Ohio Shale was deposited in the central Appalachian Basin under anoxic conditions associated with a quasi-estuarine circulation system that developed owing to massive freshwater runoff from the Catskill Delta to the northeast. As reported by Jaminski et al. (companion paper), the Cleveland Shale exhibits strong compositional variation in the stratigraphic dimension at a decimeter scale owing to (1) a variable clastic flux in association with a relatively invariant organic flux, and (2) vertical migration of H₂S from low-Fe/high-TOC to high-Fe/low-TOC intervals within the sediment column. Thus, a clastic dilution process was primarily responsible for compositional variation at this scale.

The Cleveland Shale also exhibits broad-scale stratigraphic and regional patterns of compositional variation. At a stratigraphic scale representing the entire 15-20-m-thick formation, upsection compositional changes include (1) increases in TOC from 3-5 wt% to 5-10 wt% in low-TOC hemicycles and from 5-10 wt% to 13-17 wt% in high-TOC hemicycles, (2) a decrease in the abundance of alginite and increase in that of bituminite, (3) increases in trace-element proxies for DOA, including C/S, V/Ni, and Mo/TC, and (4) a shift from an illite-quartz detrital mineral assemblage in the lower-middle part of the formation to an illite-smectite-kaolinite assemblage in the upper part of the formation. Laterally across the 210-km-long study area, compositional changes in

the distal direction include (1) an increase in TOC from 8-10 wt% to 12-14 wt% for high-TOC hemicycles, (2) little variation in TOC (ca. 5-6 wt%) in low-TOC hemicycles, (3) little variation in organic maceral types and trace-element DOA proxies across the study area, (4) little variation in detrital mineralogy in the lower and middle parts of the formation, and (5) an increase in the proportion of illite over smectite from 60%:40% proximally to 80%:20% distally.

In contrast to dm-scale cycles, which formed through a simple clastic dilution process, broad-scale stratigraphic and regional patterns of compositional variation developed through an interplay of tectonic and climatic controls within the Late Devonian central Appalachian Basin. Stratigraphic and geographic changes in TOC are inferred to be due to the same dilution process responsible for dm-scale cyclicity, i.e., influx of large quantities of siliciclastics from the Catskill Delta to the northeast. The type and quality of organic matter vary little laterally but change upsection in a manner consistent with a two- to four-fold decrease in sedimentation rates. With regard to detrital mineralogy, dominance of an illite-quartz assemblage in the lower-middle part of the formation reflects rapid influx of clastics derived through physical weathering during active uplift of the Acadian Orogen, whereas dominance of an illite-smectite-kaolinite assemblage in the upper part of the formation reflects an increase in chemical weathering, probably associated with increased humidity following termination of active uplift. Coeval changes in relative sea-level elevation within the central Appalachian Basin were controlled by thrust loading in the Acadian Orogen. The lower-middle part of the Cleveland Shale represents a major transgression and rise of the mid-water pycnocline, whereas the upper part of the Cleveland and the overlying the Bedford-Berea succession were deposited during a tectonic relaxation phase characterized by clastic influx and forced regression.

FIGURE CAPTIONS

FIG. 1. Location map for the three study cores in Ohio and Kentucky.

FIG. 2. Late Devonian paleogeography (from Witzke and Heckel 1988).

FIG. 3. Gray-scale density records over the full stratigraphic range of the Cleveland Member of the Ohio Shale in each study core. Three 20-cm-thick intervals (small rectangles) were chosen for detailed analysis in each core; compositional data for intervals OHRS 5/19/2 and 5/25/15-16 are shown in Figure 4. This hierarchical sampling strategy permitted analysis of compositional variation at both a fine (cm) and coarse (>m) scale. Correlation between study units (dashed lines) is possible on the basis of characteristic GSD and geochemical features (e.g., high V zone).

FIG. 4. Compositional data for two dm-scale cycles in the Cleveland Shale (OHRS 5/19/2 and OHRS 5/25/15-16; see Figure 3 for cycle locations). GSD values correlate negatively with TC (a proxy for TOC) and positively with TS (a proxy for Fe-sulfides). High-TC intervals are characterized by proportionately less alginite and more bituminite and by lower values for DOA indices (e.g., Mo/TC and V/Ni) than for low-TC intervals. Detrital components vary little within dm-scale cycles but exhibit substantial variation at a formation scale.

FIG. 5. Sulfur compound data for cycle OHRS-5/25/06-07. (A) Concentration in wt% of total carbon (TC; Leco analysis). (B) Concentrations in wt% of total sulfur (TS; Leco analysis), pyritic sulfur (S_{pyrite} ; chromium reduction analysis), and non-pyritic sulfur ($S_{\text{non-pyrite}}$; by difference). (C) Degree-of-pyritization values calculated from concentrations of total sulfur ($\text{DOP}_{\text{total}}$) and pyritic sulfur (DOP). (D) Measured concentrations of total Fe (XRF) and acid-soluble Fe (HCl dissolution and photospectrometer absorbance), and calculated stoichiometric concentrations of pyritic Fe based on total sulfur ($\text{Fe}_{\text{py}}(\text{TS})$) and pyritic S (Fe_{py}).

FIG. 6. Broad-scale stratigraphic-geographic variation in organic macerals. Note (1) dominance of bituminite + alginite over inertinite + vitrinite in all cores, (2) a progressive upsection increase in bituminite at the expense of alginite in the OHRS-5 and OHDW-1 cores, and (3) a distal increase (KEP-3 core) in the proportion of bituminite over alginite.

FIG. 7. Broad-scale stratigraphic-geographic variation in redox-sensitive trace elements (Ni vs. V; concentrations are normalized to TC to avoid effects associated with variation in organic matter abundance). Note (1) the linear Ni-V relation and zero Y-intercept for samples from the lower part of the Cleveland Shale (triangles), suggesting that Ni and V in these samples is largely of detrital origin, (2) a significant increase in the proportion of V over Ni in samples from the middle (diamonds) and upper (squares) parts of the formation, suggesting enhanced uptake of V as a consequence of low-oxygen conditions. No geographic trend is apparent in the data. See Figure 8 for symbols.

FIG. 8. Broad-scale stratigraphic-geographic variation in detrital mineralogy (as proxied by $\text{Al}_2\text{O}_3^*/\text{SiO}_2^*$ vs. K_2O^*). Note (1) samples from the lower and middle parts of the Cleveland Shale (triangles and diamonds) are composed of ca. 60% illite and 40% quartz and exhibit little compositional variation, and (2) samples from the upper part of the formation (squares) are composed of 60-80% illite and 20-40% smectite and exhibit a strong lateral gradient (with a distal increase in the proportion of illite). The inset in main figure illustrates mean endmember compositions for illite and smectite (ellipsoids; ± 1 standard deviation) based on published analyses from Grim (1968) and Weaver (1989). The key at right identifies stratigraphic position of samples.

FIG. 9. Broad-scale stratigraphic-geographic variation in clay mineral abundance. Note (1) upsection increase in kaolinite + chlorite over illite + smectite, and (2) possible proximal increase in kaolinite + chlorite over illite + smectite (n.b., uncertain owing to insufficient data for OHDW-1).

FIG. 10. Regional variation in clastic composition (A) and DOA indices (B).

FIG. 11. Stratigraphic model for Cleveland Shale deposition.

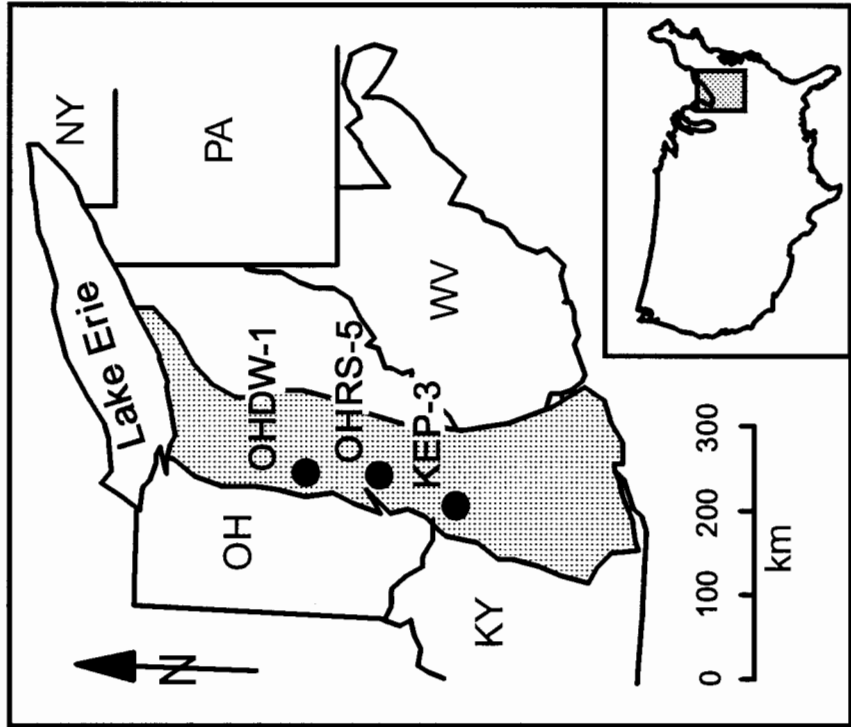
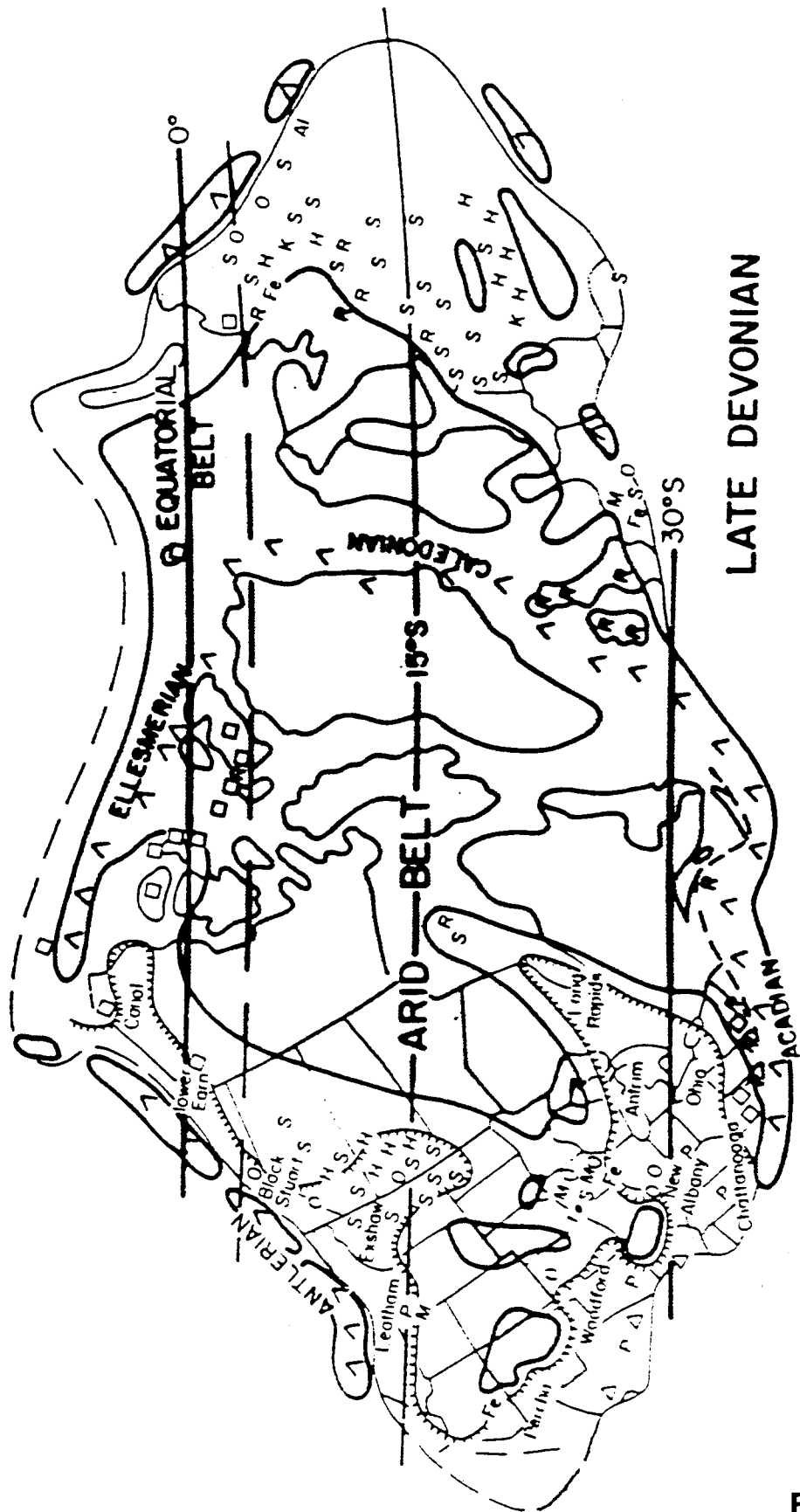


FIGURE 1



LATE DEVONIAN

FIGURE 2

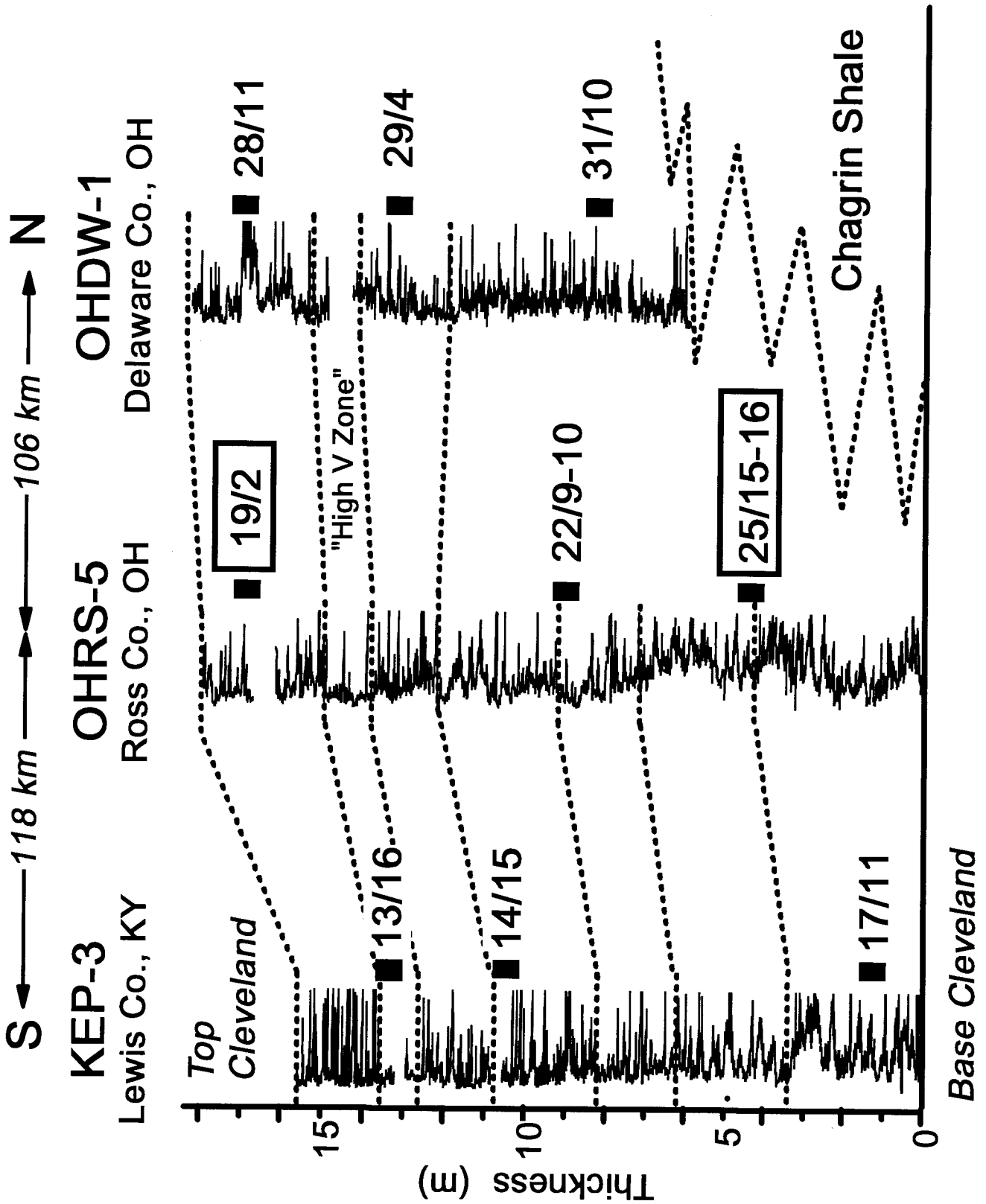


FIGURE 3

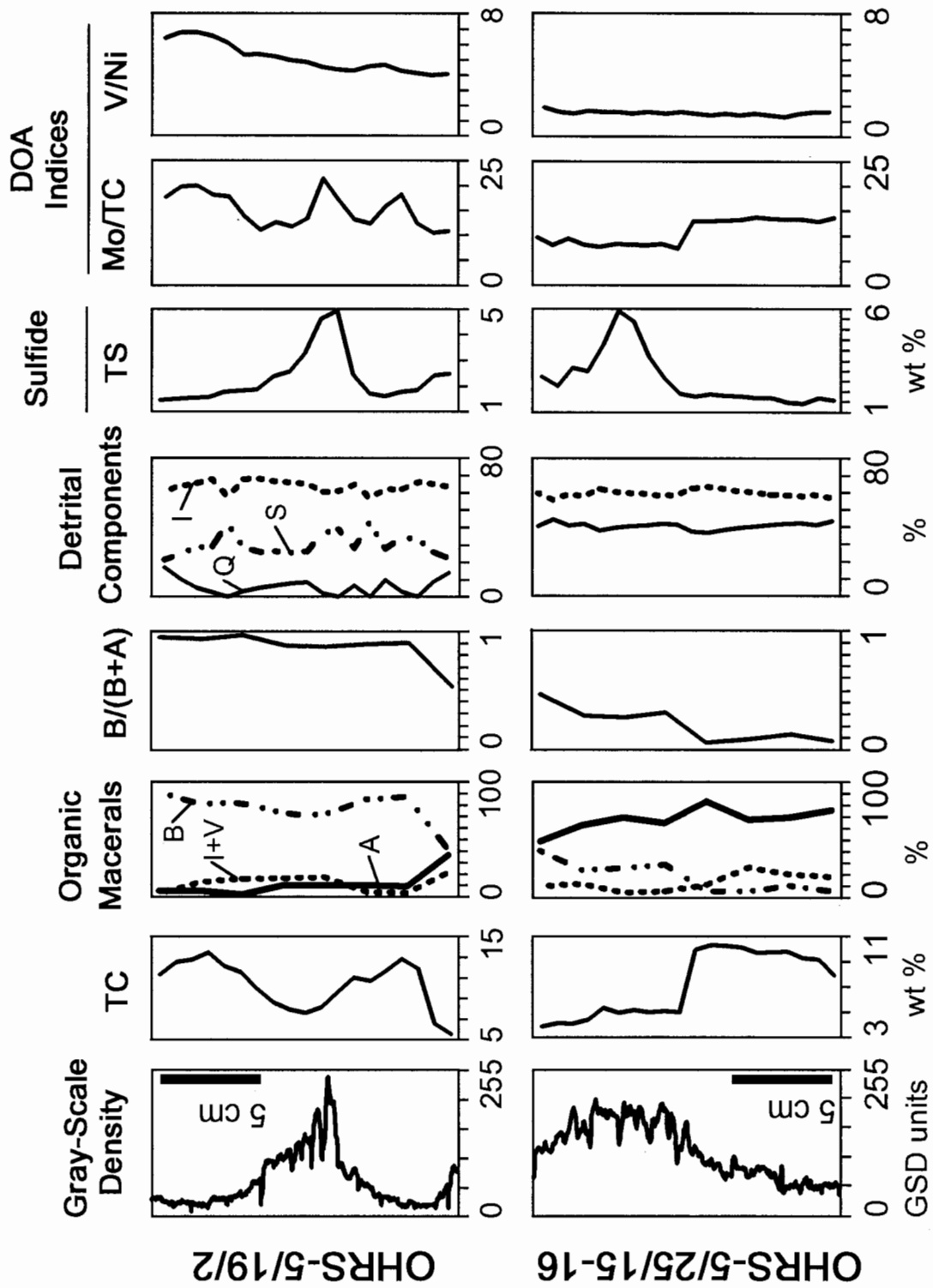


FIGURE 4

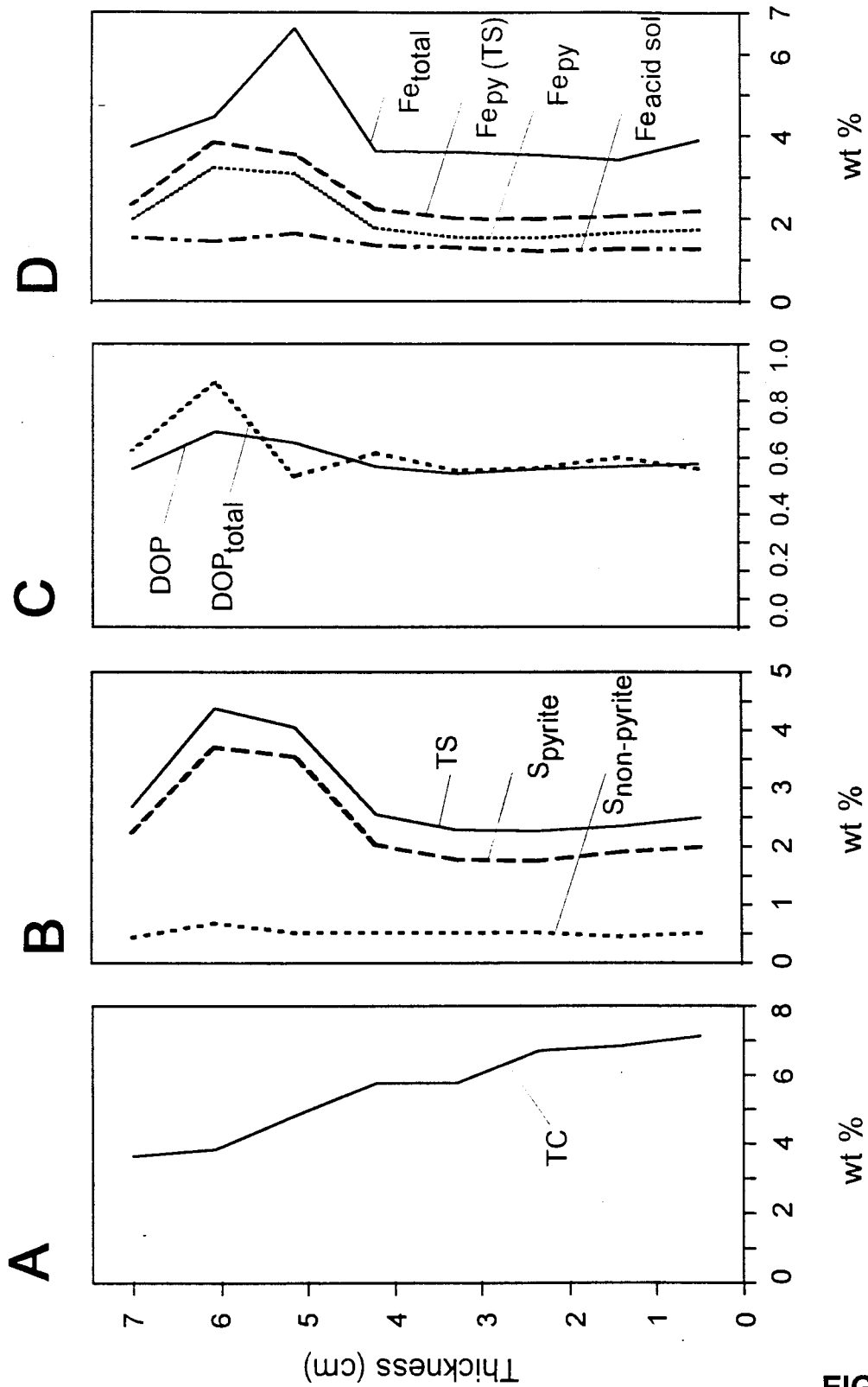


FIGURE 5

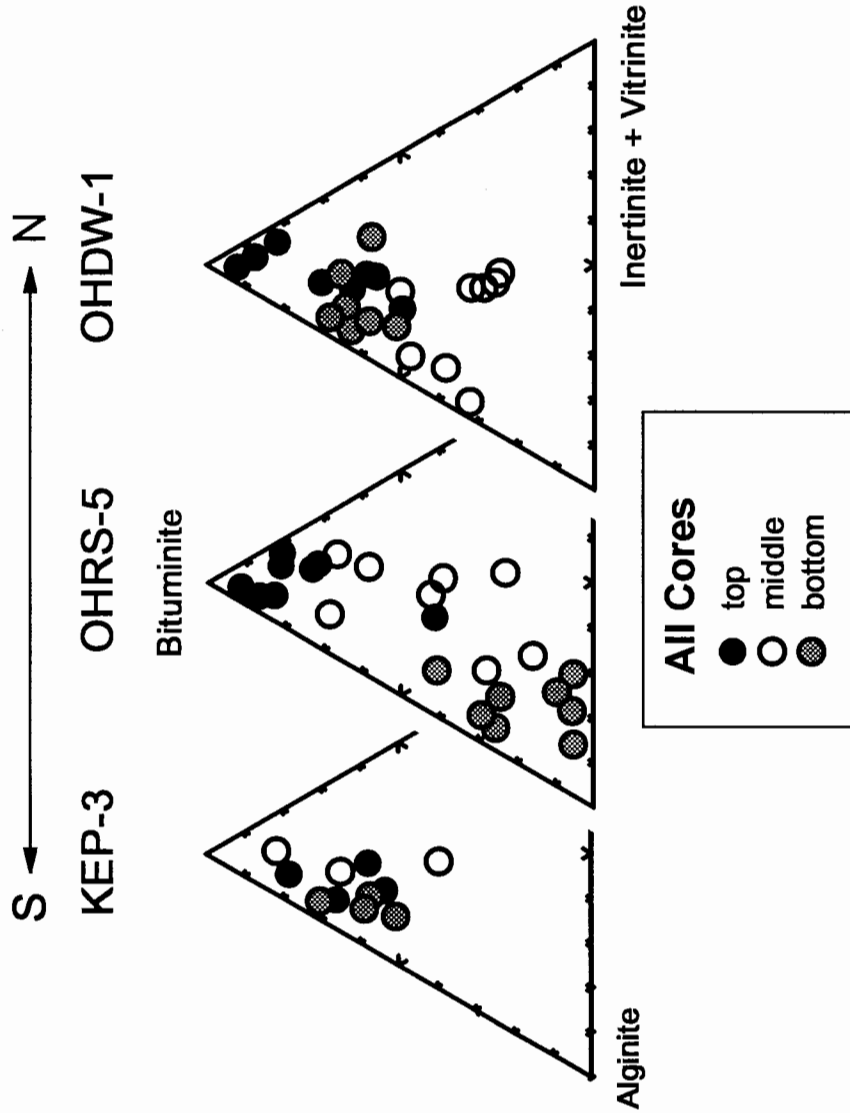


FIGURE 6

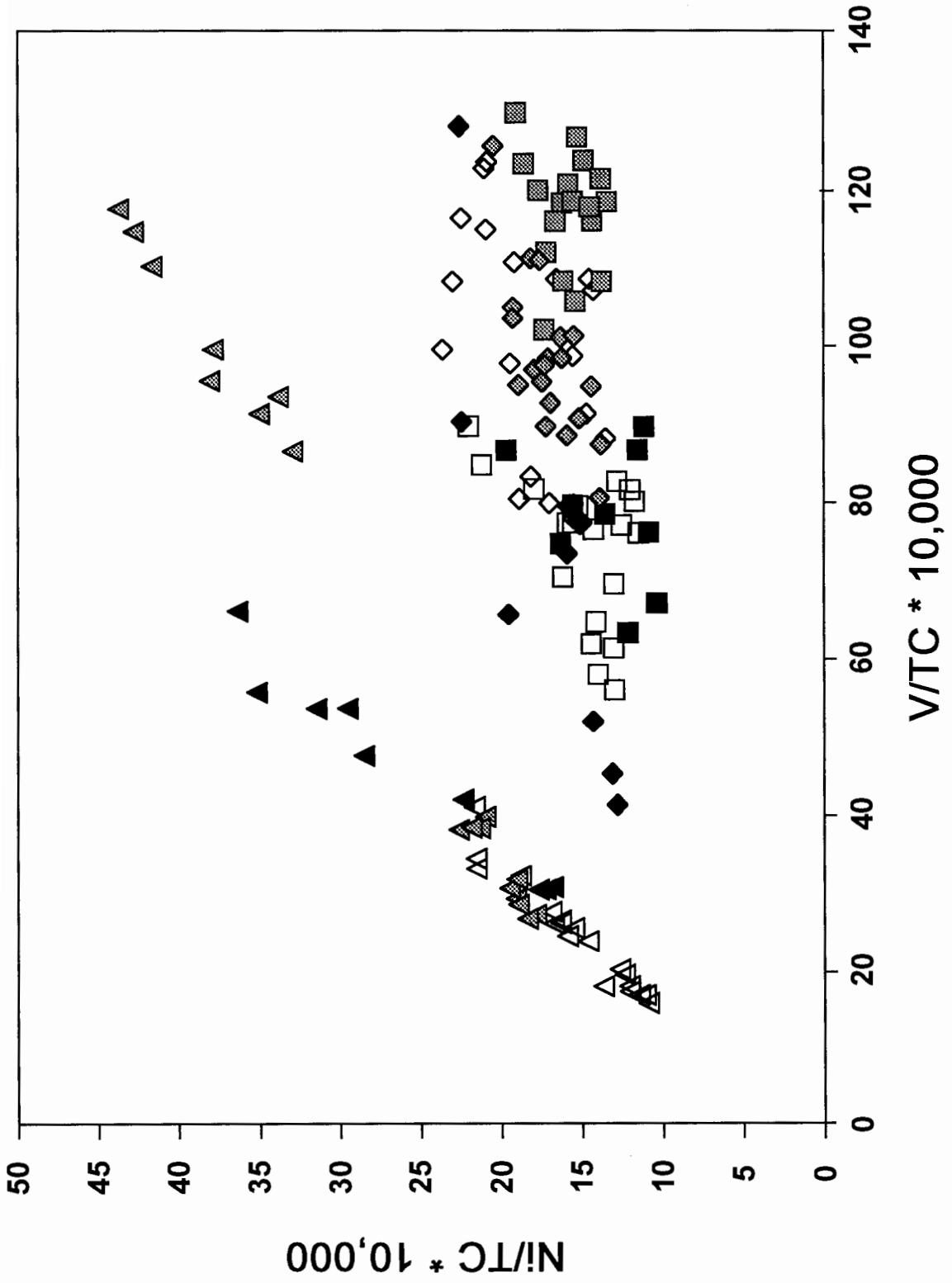


FIGURE 7

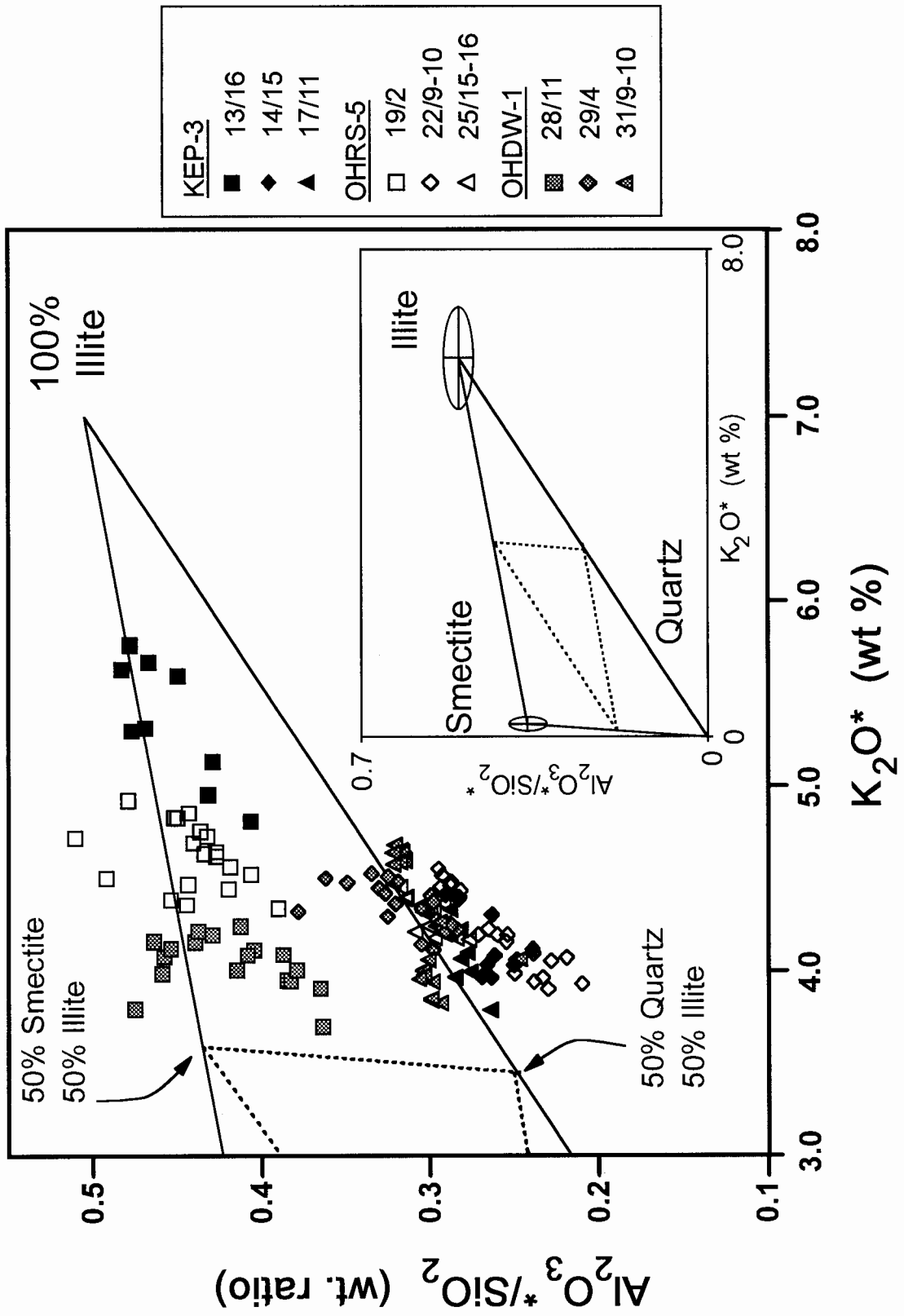


FIGURE 8

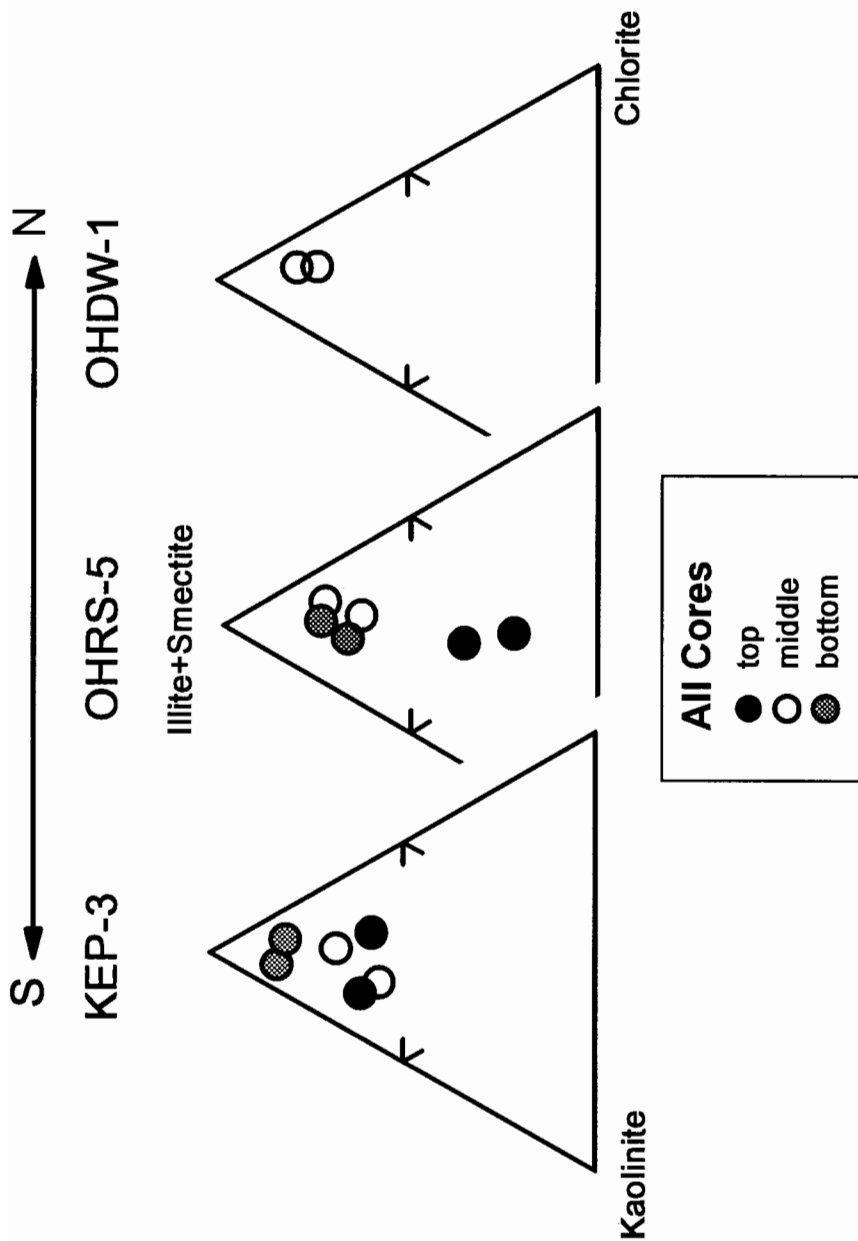
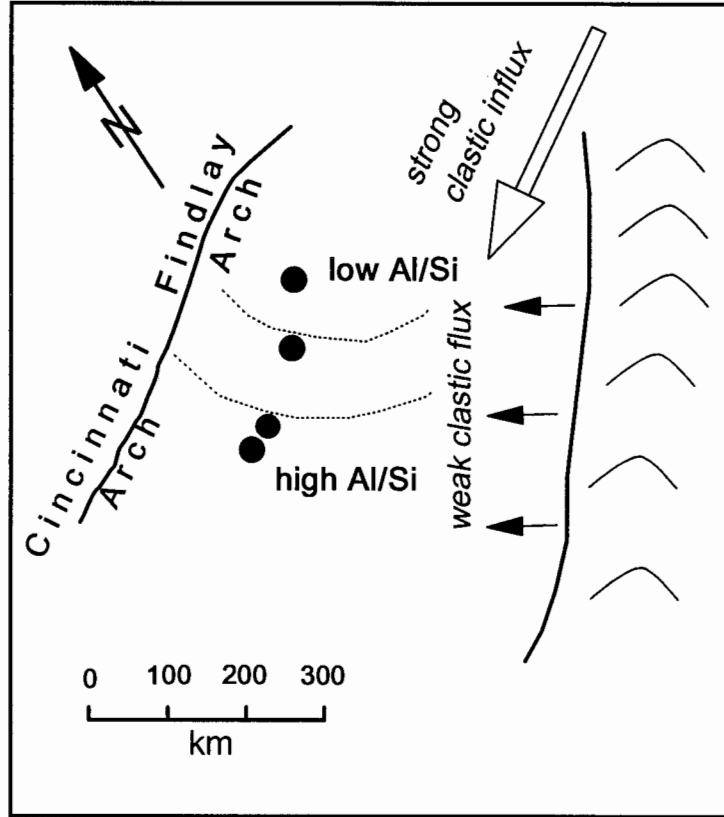


FIGURE 9

A. Clastics



B. DOA

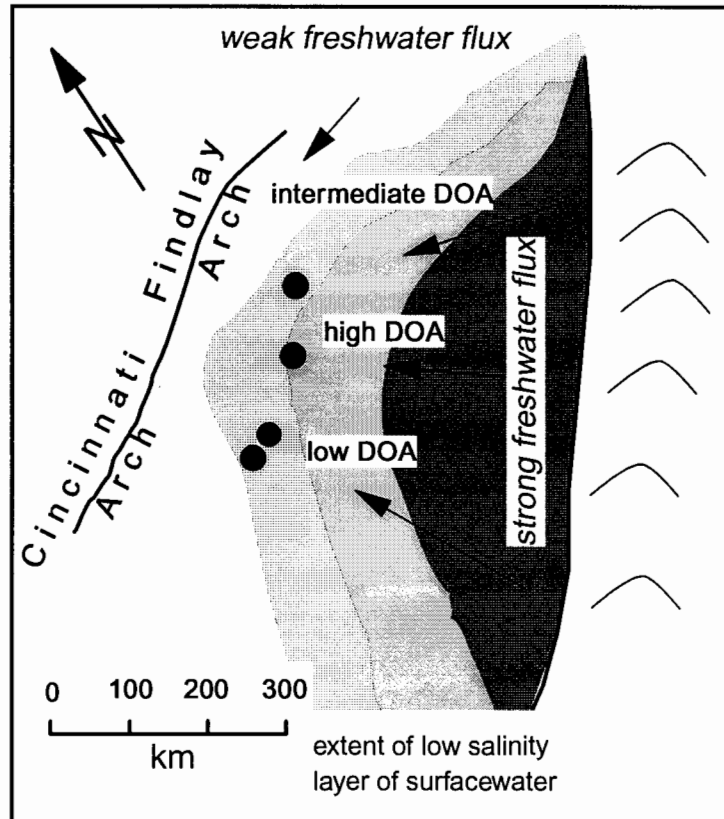


FIGURE 10

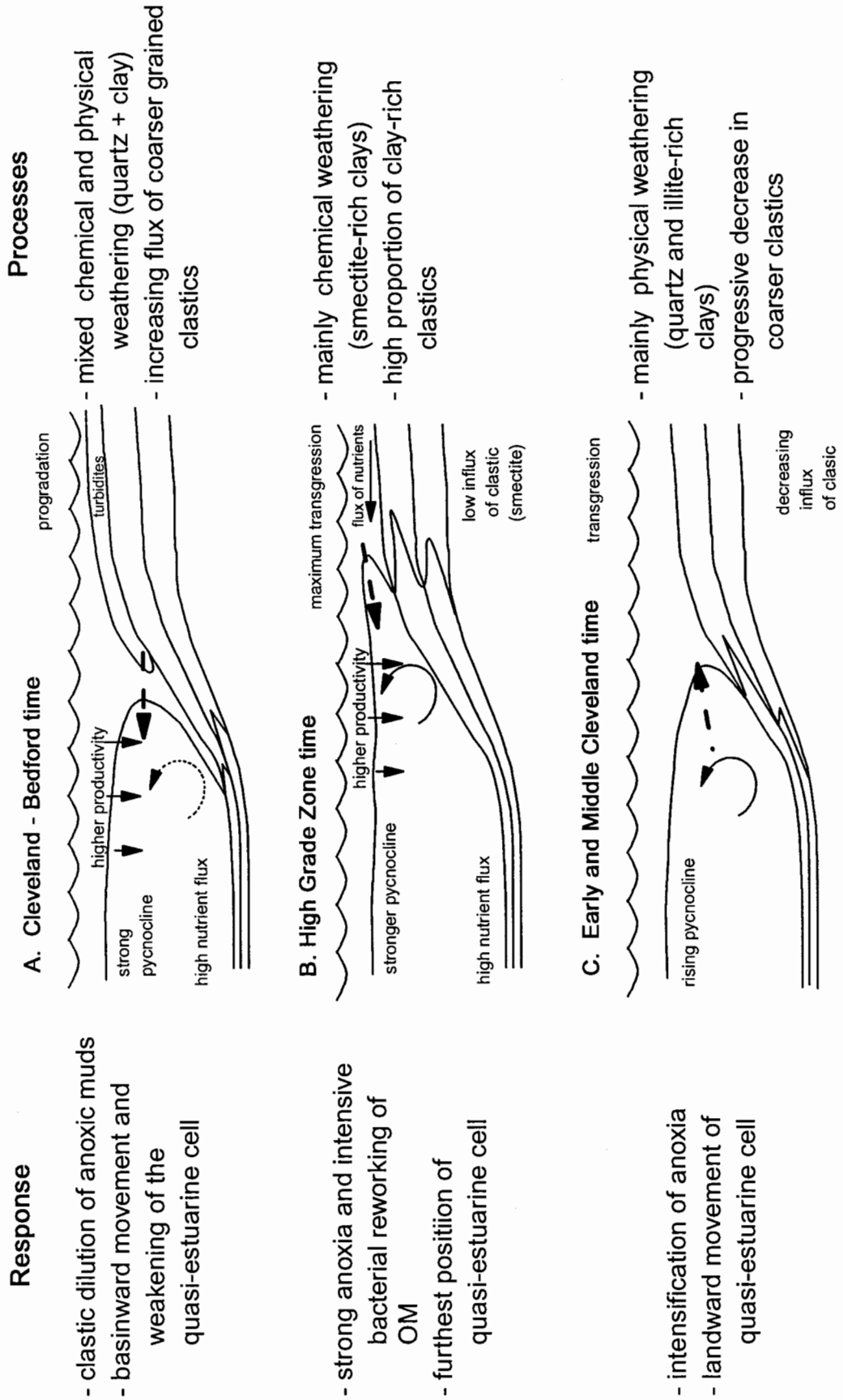


FIGURE 11